Transitional flow of a yield-stress fluid in a pipe: Evidence of a robust coherent structure

A. Esmael and C. Nouar*

LEMTA UMR 7563 CNRS - Nancy Université, 2 Avenue de la Foret de Haye, Boîte Postale 160, 54504 Vandoeuvre, France

(Received 23 October 2007; revised manuscript received 10 February 2008; published 30 May 2008)

In two independent articles, Escudier and Presti [J. Non-Newtonian Fluid Mech. **62**, 291 (1996)] and Peixinho *et al.* [J. Non-Newtonian Fluid Mech. **128**, 172 (2005)] studied experimentally the flow structure of a yield stress fluid in a cylindrical pipe. It was observed that the mean, i.e., time-averaged, velocity profiles were axisymmetric in the laminar and turbulent regimes, and presented an increasing asymmetry with increasing Reynolds number in the transitional regime. The present paper provides a three-dimensional description of this asymmetry from axial velocity profiles measurements at three axial positions and different azimuthal positions. The observed transitional flow suggests the existence of a robust nonlinear coherent structure characterized by two weakly modulated counter-rotating longitudinal vortices. This new state mediates the transition between laminar and turbulent flow.

DOI: 10.1103/PhysRevE.77.057302 PACS number(s): 47.27.nf, 47.20.−k

INTRODUCTION

Understanding the mechanism of transition from laminar to turbulent flow of Newtonian fluids has been an ongoing quest for more than a century. It is only during this last decade that considerable advances have been made with the discovery of new numerical solutions that are believed to constitute the skeleton of the turbulent attractor. For Newtonian fluid flow in a pipe of circular cross section, based on the self-sustained-process (SSP) theory developed by Waleffe [1] and the subsequent nonlinear continuation approach [2], a family of three-dimensional traveling waves that propagate at a constant phase speed in the streamwise direction were discovered by Faisst and Eckhardt [3] and Wedin and Kerswell [4]. These traveling waves (TW's) originate in saddle-node bifurcations and are immediately linearly unstable. They are dominated by pairs of downstream vortices and streaks and are very similar to the coherent structures observed experimentally in equilibrium puffs [5]. TW's of one-fold through sixfold symmetries have been identified numerically, but only twofold, threefold, and fourfold TW's are observed experimentally below a Reynolds number $\mathrm{Re}=(\rho U_B D)/\mu=3000$, where ρ is the fluid density, U_B is the bulk velocity, and $D=2R$ is the pipe diameter. Very recently, asymmetric TW's composed by two rolls in the cross section were computed [6–8].

Concerning the transition to turbulence for non-Newtonian fluids flows, very little is available in the literature, despite the importance of this problem in the design and control of several industrial processes such as in oil-well cementing, extrusion of molten polymers, paper coating, etc. Nevertheless, the existing literature reveals an interesting and yet unexplained effect: In a certain range of Reynolds numbers, the mean flow presents an asymmetry, while in the laminar and turbulent regimes the flow is axisymmetric. Here, mean refers to time-averaged. Independent observations of this asymmetry have been made by Escudier and Presti [9] and Peixinho *et al.* [10]. These two groups recently jointly published these and additional observations in [11] to highlight the effect. It was also clearly indicated in [11] that this asymmetry is not a consequence of the Coriolis force arising from the Earth's rotation. Likewise, the temperature gradients as well as the longitudinal curvature of the pipe are too weak to modify the velocity profile. Therefore, the asymmetry of the velocity profiles observed in [9,10] is a consequence of a fluid-dynamical mechanism rather than an experimental artifact. This conclusion is supported by two different studies: (i) an experimental study of Eliahou *et al.* [12] on the transitional pipe flow for Newtonian fluid and (ii) direct numerical simulation of the weakly turbulent pipe flow of shear thinning fluid performed by Rudman *et al.* [13]. In the first study, an asymmetric distortion of the mean velocity profiles is observed only when a high amplitude asymmetric perturbation is imposed. In the second one, the authors indicate that for sufficiently shear thinning behavior (power-law fluid with $n=0.5$), "the active region of the flow continually moves along the pipe and appears to preferentially occur at one azimuthal location for extended times."

A three-dimensional description of the asymmetry is given in this paper. The measurements performed in the transitional flow allowed to highlight the existence of a nonlinear robust coherent structure. Its contribution to structuring the transition process will be discussed. As a starting point, the linear stability of Hagen-Poiseuille flow of a yield stress fluid is considered.

We recall that the one-dimensional shear flow of a yield stress fluid is characterized mainly by the presence of a plug zone of radius r_0 moving as a rigid body. In the sheared zone, between the wall at $r=R$ and the yield surface at $r=r_0$, the effective viscosity μ decreases nonlinearly with increasing shear rate. Actually, μ is infinite at the yield surface and decreases when approaching the wall. In the following, it is assumed that the rheological behavior of the fluid can be described by the Herschel-Bulkley model. For unidirectional shear flow with velocity U_ℓ in the z direction, the relationship between the shear stress τ_{rz} and the velocity gradient dU_ℓ/dr is

$$\tau_{rz}=\mathrm{sgn}(dU_\ell/dr)\,\tau_0+K\left|\frac{dU_\ell}{dr}\right|^{n-1}\frac{dU_\ell}{dr}\Leftrightarrow|\tau_{rz}|\geq\tau_0,$$

*Author to whom correspondence should be addressed.

$$dU_\ell/dr = 0 \Leftrightarrow |\tau_{rz}| \leq \tau_0,$$

where τ_0 is the yield stress, n is the flow behavior index, and K is the consistency index. The axial velocity profile $U_\ell(r)$ is given by

$$\frac{U_\ell(r)}{U_B} = \begin{cases} \dfrac{U_{\ell\,\max}}{U_B}, & 0 \leq r \leq r_0, \\ \dfrac{U_{\ell\,\max}}{U_B}\left[1 - \left(\dfrac{r-r_0}{R-r_0}\right)^{\frac{n+1}{n}}\right], & r_0 \leq r \leq R, \end{cases} \tag{1}$$

with

$$\frac{U_{\ell\,\max}}{U_B} = \frac{n}{n+1}\left(\frac{\mathrm{Hb}}{a}\right)^{1/n}(1-a)^{(n+1)/n},$$

where U_B is the bulk velocity, $a = r_0/R$, and $\mathrm{Hb} = \tau_0 R^n / K U_B^n$ is the Herschel-Bulkley number. The base flow is governed by two parameters, n and a or n and Hb. The dependence of a with respect to n and Hb can be found using the continuity equation in integral form [10].

LINEAR THEORY

The linear stability of Hagen-Poiseuille flow of Herschel-Bulkley fluid to infinitesimal disturbances is studied for different values of n and Hb. Using the normal-mode approach, the disturbance fields are assumed to be of the form $\psi(r)\exp[i(\alpha z + m\theta - \omega t)]$, where α and m are, respectively, the axial and azimuthal wave numbers. The numerical results lead to the conclusion that the flow configuration $(0,0,U_\ell(r))$ is linearly stable for all Reynolds numbers $\mathrm{Re} = \rho U_B D/\mu_w$, where μ_w is the wall shear viscosity. This result could have been anticipated on the basis of [14].

When a small perturbation composed by a weighted combination of linear eigenfunctions is considered, there is a potential for a short-time amplification of the energy perturbation. This is a consequence of the non-normality of the linear stability operator, the eigenfunctions being nonorthogonal under the energy norm. The transient evolution of the disturbance kinetic energy is determined following the same methodology as in [15]. For a given Fourier mode, the maximum amplification of the kinetic energy at any instant in time is denoted by G and the maximum of G for all pairs (α,m) is denoted G^{opt} and is reached by the optimal perturbation at a specific time t^{opt}. At the same dynamical and rheological parameters as in the experimental tests ($\mathrm{Re} = 2420, n = 0.5, a = 0.1$), the numerical results show that the strongest linear transient growth is obtained for a traveling-wave perturbation with $m=2$ and $\alpha = 1.20$, giving $G^{\mathrm{opt}} = 96.14$ reached after 8.98 time units R/U_B. The perturbation gains energy due to the inviscid Orr-liftup mechanism. For comparison, in the case of streamwise independent perturbation with $m=1$, we have $\sup_{t\geq 0} G \approx 31.9$ reached at $t=25.2$. The cross-flow velocity vectors and the corresponding optimal streaks are represented in Fig. 1.

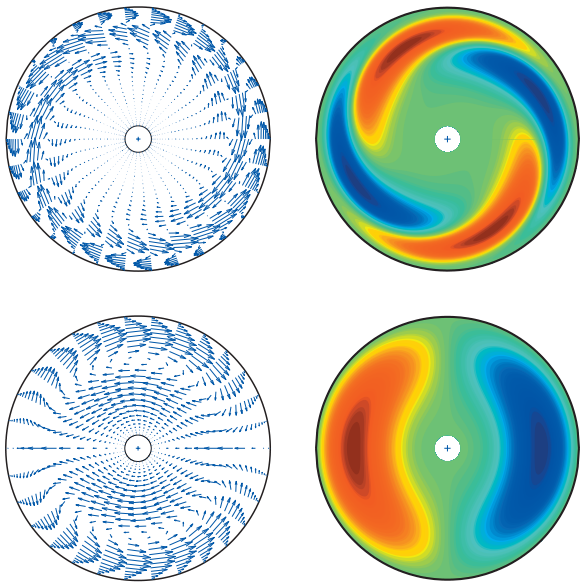

FIG. 1. (Color) Cross flow in the $(r\text{-}\theta)$ section and streaks distribution at $\mathrm{Re} = 2420$, $n = 0.5$, and $a = 0.1$. (Top) Optimal perturbation with $m=2$ and $\alpha = 1.20$; (bottom) streamwise independent vortices with $m=1$. The red and blue zones correspond, respectively, to the fast and low streaks. The central gray zone is the theoretical plug zone.

EXPERIMENTAL SETUP, INSTRUMENTATION, AND TESTED FLUIDS

Full details of the flow facility and instrumentation have been given in [10] and so only a brief description is given here. Measurements were carried out in a Plexiglas tube of internal diameter equal to 30 mm and 4.20 m long. This tube is longer than the entry length L_e necessary for the laminar flow to fully develop in all experiments carried out [16]. The velocity measurements were performed using a Dantec FlowLite system with a measuring volume 651 μm in length and 77 μm in diameter. The working fluid is a 0.2 wt.% aqueous solution of Carbopol 940. It is widely used as a model yield-stress fluid because of its stability and transparency. The rheological measurements were made with a controlled torque rheometer. It is found that for a large range of shear rates ($0.1 \leq \dot{\gamma} \leq 3 \times 10^3\ \mathrm{s}^{-1}$), the flow curve is very well fitted by the Herschel-Bulkley model: $\tau = \tau_0 + K\dot{\gamma}^n$.

RESULTS AND DISCUSSION

A set of the measured mean axial velocity profiles at $z = 122$ D from the entrance section in laminar, transitional, and turbulent regimes is represented in Fig. 2(a). At each radial position, the mean velocity is extracted from more than 8×10^4 validated data recorded during 3 mn. The measurements were done along a diameter in the horizontal median plane. As indicated above, the Reynolds number is defined with the wall shear viscosity, calculated using the Herschel-Bulkley model fit at the wall shear stress estimated from the pressure drop measurements. The continuous line is an averaged mean velocity profile $\bar{U}(r)$ obtained by taking

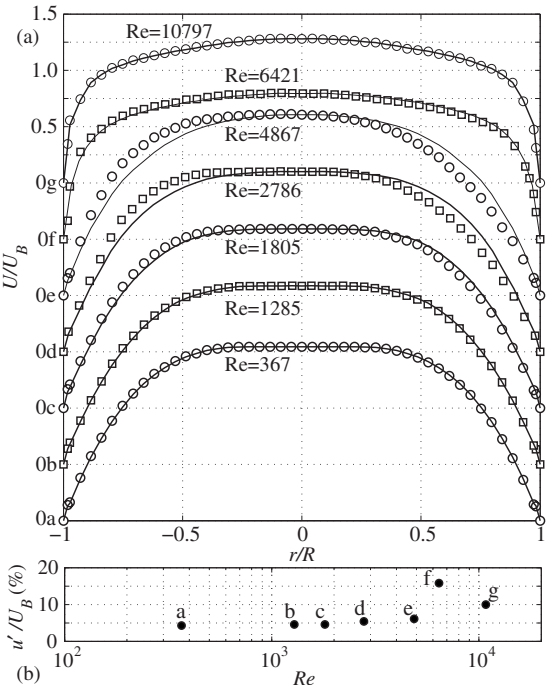

FIG. 2. (a) Mean axial velocity profiles at different Reynolds number, $\tau_0=9.75$ Pa, $K=3.82$ Pa s^n, $n=0.47$; (b) axial velocity fluctuations level $u'(\mathrm{rms})/U_B$ vs Re at $r/R=0.8$. The symbols denote the experimental data and the continuous line is an average velocity profile obtained by taking the average of the velocity data from either side of the centerline.

the average of the mean velocity data from either side of the centerline. An indication on the flow regime is given by the near-wall $(r/R=0.8)$ axial velocity fluctuations level $u'(\mathrm{rms})/U_B$ vs Re displayed in Fig. 2(b). In the laminar regime (Re=367 and 1285), the axial velocity profiles are symmetric and in very good agreement with the theoretical profiles. In the transitional regime (Re=1805–4867), an increasing asymmetry of the axial velocity profile with increasing Re is observed. The profiles Re=6421 and 10797 are symmetric; they correspond, respectively, to the maximum of (u'/U_B) and turbulent flow.

In order to provide a three-dimensional description of the asymmetry observed in the transitional regime, axial velocity profiles are measured at three axial positions: $z=20$ D (near the entrance section), $z=54$ D (middle of the pipe), and $z=122$ D, and four azimuthal positions $\theta=0$ (horizontal plane), $\pm\pi/4$, and $\pi/2$. The anticlockwise orientation is adopted and the Reynolds number is fixed at Re=2420. The obtained mean velocity profiles $U(r,\theta,z)$ are then written as the superposition of an averaged mean axial velocity profile $\bar{U}(r,z)$ and a streak $U_s(r,\theta,z)$. The azimuthal variation of U_s/U_B at different radial positions and at the three axial positions indicate clearly that $\frac{U_s(r,\theta,z)}{U_B}$ is well described by the relation $\frac{U_s(r,\theta,z)}{U_B}=A(r,z)\cos(\theta+\phi)$. As an example, Fig. 3 shows U_s/U_B versus θ at $r/R=0.72$. Even if currently we cannot conclude about the saturation of the streaks, it is worthwhile to note that the phase ϕ remains invariant along the pipe, and depends probably only on the inlet conditions. It is thus possible to draw the contours of iso-U_s in a cross

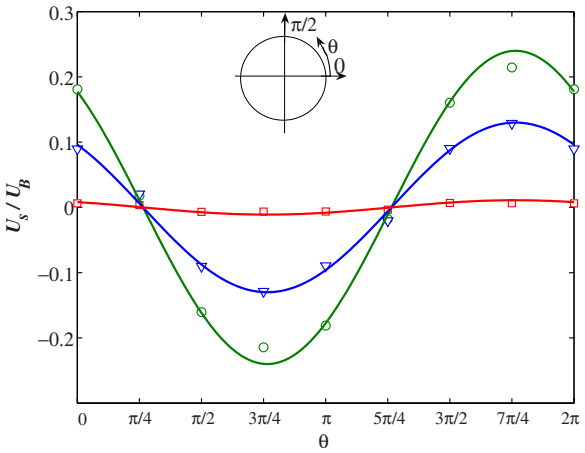

FIG. 3. (Color online) Azimuthal variation of the streak velocity at Re=2420, $r/R=0.72$, and at the three axial positions: $z=20$ D (square), $z=54$ D (nabla), and $z=122$ D (circle).

section of the pipe, at each axial position considered. The result of this procedure is given in Fig. 4. The red color indicates regions where the flow of the fluid in the direction of the pipe is faster than the averaged mean profile, while blue denotes regions that are slower than the averaged mean flow. These streaks suggest the existence of a coherent structure characterized by two counter-rotating longitudinal vortices, similar to those represented in Fig. 1 (bottom frames). Slow flow is advected from the wall toward the blue zone and fast flow is advected toward the red zone. As in the case of the self-sustained cycle proposed by Waleffe [1], one can anticipate that a shear flow instability of the streaks regenerates the vortices. The visualization of this instability, for instance from the velocity-time history signal displayed in Fig. 5(c), is not possible. Indeed, the frequency power spectra of the velocity fluctuations indicate that the dominant frequencies are practically less than 1 Hz without revealing any particular frequency. Therefore, this nonlinear state is not a simple periodic traveling wave. It is worthwhile to note that there is a highly viscous zone near the axis where u'/U_B remains at the same level as in laminar regime [Figs. 5(a) and 5(b)]. With increasing Reynolds number, the diameter of this zone decreases to zero. In our experiments, u'/U_B on the axis starts to increase from $\mathrm{Re}=\mathrm{Re}_{c2}\approx 4000$ with the detection of the first turbulent spots, while the asymmetry is ob-

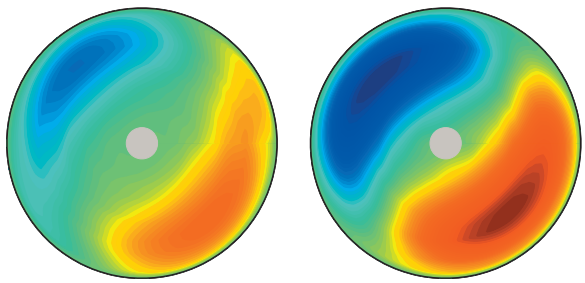

FIG. 4. (Color) Cross section in (r,θ) at two axial positions $z/D=54$ and 122 shows contours of iso-$(U-\bar{U})/U_B$, with the fast streaks (red/dark bottom) and low streaks (blue/dark top). Re =2420, $n=0.5$, and $a=0.1$.

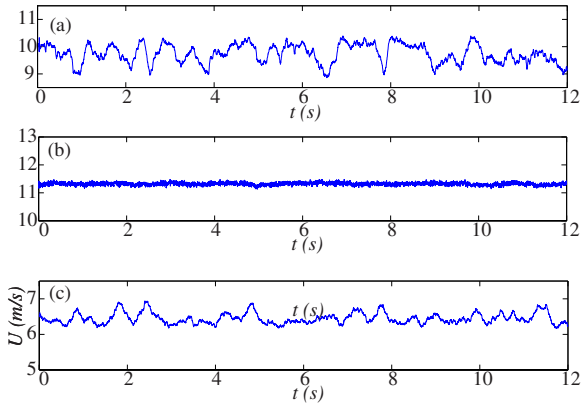

FIG. 5. (Color online) Instantaneous axial velocity plots at Re=2420, z=122 D, n=0.5, and a=0.1. (a) r=0; (b) r/R=0.3, $\theta=7\pi/4$; and (c) r/R=0.72, $\theta=7\pi/4$.

served from $\mathrm{Re}=\mathrm{Re}_{c1}\approx 1800$. From $\mathrm{Re}=\mathrm{Re}_{c2}$, the flow cycles between the turbulent regime and the asymmetric state described above. The significance of the results described here is well analyzed in the framework of dynamical system theory. We can choose to display them in a suitably defined phase subspace, such as that spanned by the rate of energy dissipation D per unit volume and the rate of energy input I per unit volume (see Fig. 6), along the lines of Biau *et al.* [17]. Steady states must fall on the line $I=D$ where the two quantities are in balance. In this subspace, the steady laminar flow is a linearly stable fixed point for all Re and a global attractor for $\mathrm{Re}<\mathrm{Re}_{c1}$. In our case, $\mathrm{Re}_{c1}\approx 1800$, so that all initial conditions are attracted to the laminar node when $\mathrm{Re}<\mathrm{Re}_{c1}$. At $\mathrm{Re}=\mathrm{Re}_{c1}$, a new state with a robust nonlinear coherent structure is selected by the flow. This new state may arise through a saddle-node bifurcation. Starting from $\mathrm{Re}=\mathrm{Re}_{c2}\approx 4000$, the basin of attraction of the asymmetric state decreases and the flow trajectory can escape from this state through a second saddle, follow this saddle's stable manifold, and move toward an upper branch solution represented by point (3). After orbiting for a while around such a solution, which corresponds to the mean turbulent flow, the flow can either return to the local attractor represented by node (2), or it can escape through yet another low-dimensional saddle toward a different region of phase space. The view just outlined, admittedly speculative, is supported by all available experimental results.

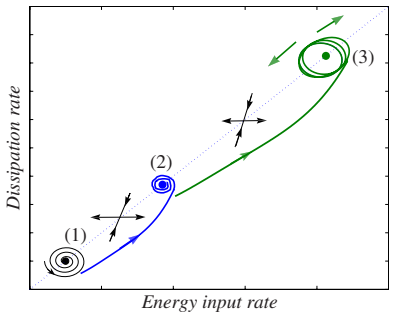

FIG. 6. (Color online) Qualitative description of the transition process in the phase diagram displaying dissipation rate versus energy input rate. Point (1) is the steady, one-dimensional laminar state, toward which the system returns spirally when $\mathrm{Re}<\mathrm{Re}_{c1}$. Point (2) represents the time-averaged value of D and I for the nonlinear asymmetric state. The upper branch state (3) represents the mean turbulent flow. The crosses with arrows sketch unstable saddle nodes. Flow trajectories are sketched for increasing values of Re.

CONCLUSION

The following conclusions can be drawn from this study: (i) Optimal disturbances are not useful to describe early stages of transition; (ii) a robust nonlinear coherent structure mediating the transition from laminar to turbulent flow exists. It persists for the whole duration of the experiments (several weeks); (iii) it is worthwhile to investigate whether this new state found here is dynamically connected to the *edge states* recently computed in the Newtonian case [6–8]; (iv) the asymmetric solutions act as local attractors in phase space. As Re is increased from zero, the basin of attraction of this asymmetric state increases, then it shrinks.

ACKNOWLEDGMENTS

The authors are very grateful to A. Bottaro, J. P. Brancher, and E. Plaut for fruitful discussions.

[1] F. Waleffe, Phys. Fluids **9**, 883 (1997).
[2] F. Waleffe, Phys. Rev. Lett. **81**, 4140 (1998).
[3] H. Faisst and B. Eckhardt, Phys. Rev. Lett. **91**, 224502 (2003).
[4] H. Wedin and R. R. Kerswell, J. Fluid Mech. **508**, 333 (2004).
[5] B. Hof, C. V. Doorne, J. Westerweel, F. Nieuwstadt, H. Faisst, B. Eckhardt, H. Wedin, R. Kerswell, and F. Waleffe, Science **305**, 1594 (2004).
[6] C. C. T. Pringle and R. R. Kerswell, Phys. Rev. Lett. **99**, 074502 (2007).
[7] T. M. Schneider, B. Eckhardt, and J. A. Yorke, Phys. Rev. Lett. **99**, 034502 (2007).
[8] B. Eckhardt, T. Schneider, B. Hof, and J. Westerweel, Annu. Rev. Fluid Mech. **39**, 447 (2007).
[9] M. P. Escudier and F. Presti, J. Non-Newtonian Fluid Mech. **62**, 291 (1996).
[10] J. Peixinho, C. Nouar, C. Desaubry, and B. Théron, J. Non-Newtonian Fluid Mech. **128**, 172 (2005).
[11] M. P. Escudier, R. J. Poole, F. Presti, C. Dales, C. Nouar, C. Desaubry, C. Graham, and L. Pullum, J. Non-Newtonian Fluid Mech. **127**, 143 (2005).
[12] S. Eliahou, A. Tumin, and I. Wignanski, J. Fluid Mech. **361**, 333 (1998).
[13] M. Rudman, H. M. Blackburn, L. J. W. Graham, and L. Pullum, J. Non-Newtonian Fluid Mech. **118**, 33 (2004).
[14] C. Nouar, N. Kabouya, J. Dusek, and M. Mamou, J. Fluid Mech. **577**, 211 (2007).
[15] P. J. Schmid and D. S. Henningson, *Stability and Transition in Shear Flows* (Springer-Verlag, New York, 2001).
[16] G. B. Froishteter and G. V. Vinogradov, Rheol. Acta **19**, 443 (1980).
[17] D. Biau, H. Soueid, and A. Bottaro, J. Fluid Mech. **596**, 133 (2008).